

Carbocation Branching Observed in a Simulation

A. L. L. East,^{*,†} T. Bucko,[‡] and J. Hafner[‡]

Department of Chemistry and Biochemistry, University of Regina, Regina, Saskatchewan S4S 0A2, Canada, and Faculty of Physics and Center for Computational Materials Science Materialphysik, Universität Wien, Sensengasse 8, A-1090 Wien, Austria

Received: March 23, 2007; In Final Form: May 22, 2007

We have observed the branching rearrangement of a straight-chain secondary carbocation ($C_9H_{19}^+$) in an ab initio molecular dynamics (AIMD) reverse-annealing (rising-temperature) simulation. The mechanism observed is one involving closed (protonated-cyclopropane) structures, previously observed in traditional geometry optimization calculations. However, the simulations give us a better understanding of the dynamics involved, leading to two advances: a simpler description of carbenium ion structures in general and the discovery of important entropy effects.

In petroleum chemistry, the catalytic cracking of unbranched hydrocarbons produces branched hydrocarbon products in substantial yields. The branching steps occur with carbocations, rather than neutral hydrocarbons, and early proposals of an involved protonated cyclopropane (PCP⁺) structure by McCaulay,¹ Brouwer,² and others have been explored by several computational chemistry studies. What remains is to understand the precise mechanistic steps involved. A two-step mechanism was computationally identified by Corma's group,³ but at least two ensuing investigations,^{4,5} involving contact of a carbocation with a catalyst, hint that chemisorption might require changes in the mechanism.

We wish to report a breakthrough in the understanding of the branching rearrangement steps. We have achieved the first molecular dynamics simulation of the branching steps that produce a tertiary carbocation (4-methyl-4-octenium ion) from a secondary one (4-nonenium ion). This simulation was unbiased, in that it used a density-functional-theory potential-energy surface, and no mode-specific reaction-driving artificialities whatsoever.⁶ From this simulation, and our additional computation of the transition states corresponding to the two observed steps, we now better understand the entropy effects on the mechanism and can present an updated description of the branching step in petroleum chemistry.

The ab initio molecular dynamics (AIMD) simulations were performed with the Vienna ab initio simulation package (VASP).¹¹ The level of theory was PW91, a gradient-corrected density functional theory (GGA DFT).¹² The calculations used Blochl's projector augmented wave technique,^{13,14} applied to pseudopotentials appropriate for GGA DFT,^{15,16} and a plane-wave basis set with an energy cutoff of 500 eV. The simulation that produced the isomerization of the nonenium ion was a condensed-phase simulation of the nonenium ion in an ionic liquid, consisting of 5 pyridinium cations ($C_5H_5NH^+$) and 6 $Al_2Cl_7^-$ ions. The liquid phase was mimicked by replicating a

TABLE 1: Highlights Observed during the Reverse-Annealing Simulation

Time (fs)	Event	Sketch
1950-1970	1 st exploration of the entrance channel to high-energy beta-scission	
4800-4820	1 st episode of PCP ⁺ structure	
4805	H-shift along PCP ⁺ "base"	
4930-5170	2 nd episode of PCP ⁺ structure	
4932	Step 1: H-shift along PCP ⁺ "side" (making sec-methyloctenium ion) from C _γ to C _β	
5060	Methyl group (C _β) side-to-side oscillation: θ _{βγ} = 90° turning point	
5120	Methyl group (C _β) side-to-side oscillation: θ _{βα} = 90° turning point	
5170	Methyl group (C _β) side-to-side oscillation: θ _{βγ} = 90° surpassed (end of PCP ⁺)	
5258	Step 2: 1,2-H-shift from C _α to C _γ (making tert-methyloctenium ion)	
5368	1,2-H-shift to C _α (making a new sec-methyloctenium ion)	
5400	1,2-H-shift from C _α (re-establishing tertiary ion)	

[†] University of Regina.

[‡] Universität Wien.

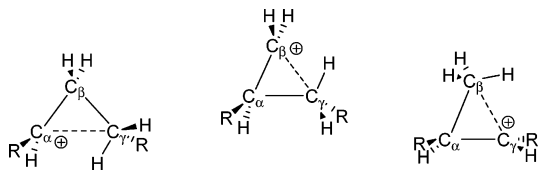


Figure 1. Branching step of an unbranched secondary carbenium ion. The rise from left intermediate to center transition state involves a 60° internal rotation of the “alkyl” group at the γ carbon, which formally rearranges the C–C bonds and creates a closed primary-carbenium ion transition state. The fall from transition state to right intermediate involves an *H-atom shift* from the γ to β carbon atoms, which formally creates a closed secondary carbenium ion. As the diagram suggests, the atom and electron-density shifts during this step are not dramatic. (Both the intermediates and the transition state could variously be called edge-protonated or corner-protonated PCP⁺ structures, making such a naming system a semantic exercise.)

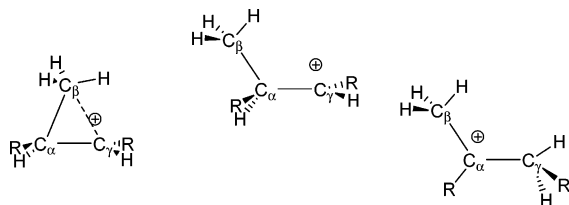


Figure 2. Second step in the branching of an unbranched secondary carbenium ion. The rise from left intermediate to center transition state involves a *ring opening* from a closed secondary methyloctenium ion to an open one. The fall from transition state to right intermediate involves an *H-atom shift* from α to γ carbon atoms, which converts the secondary carbenium ion to a tertiary one. The $\alpha\beta\gamma$ labels are taken to be in the same positions as in Figure 1, for continuity.

unit cell using periodic boundary conditions, and calculations were restricted to the gamma point. Each atom was given an isotope-averaged mass (e.g., 35.453 amu for Cl), except for H (mass 1.000 amu). The cell was chosen to have a width of 13.90 Å, a 4% volume expansion relative to that required for a $(\text{C}_5\text{H}_5\text{NH}^+)_6(\text{Al}_2\text{Cl}_7^-)_6$ simulation at the experimentally observed density of 1.476 g cm^{-3} .¹⁷ Simulations were performed with the NVT (canonical) ensemble, using a Nosé thermostat¹⁸ set for a thermal oscillation every 40 time steps (SMASS=0), and a Verlet velocity algorithm¹⁹ with a time step of 1 fs.

The sequence of simulations began with a constant-temperature run, for 3 ps at 773 K, during which three 1,2-H-shifts were observed on the nonenium ion. It continued with another 3 ps at 973 K, during which five or six similar shifts were observed on this ion, as well as a brief 75 fs episode of interanion reactions ($2 \text{ Al}_2\text{Cl}_7^- \rightarrow \text{AlCl}_4^- + \text{AlCl}_3 + \text{Al}_2\text{Cl}_7^- \rightarrow \text{AlCl}_4^- + \text{Al}_3\text{Cl}_{10}^- \rightarrow 2 \text{ Al}_2\text{Cl}_7^-$). The simulation then continued using a reverse simulated-annealing algorithm, steadily increasing the temperature at a baseline rate of 0.2 K per femtosecond.

We categorize carbenium ion structures as either *open* (all connected $\theta_{\text{CCC}} > 90^\circ$, as in structures 1–3 and 5–8 of ref 20) or *closed* (some $\theta_{\text{CCC}} < 90^\circ$, as in structures 4 and 10 of ref 20). Open structures, depending on the degree of branching, may or may not feature H-atom bridging. Closed structures include those that have been variously described as either alkyl-bridged or PCP⁺. Debates about PCP⁺ structures (intermediate vs transition state, edge-protonated vs corner-protonated) have a long history, likely due to the fact that computed minimum-energy structures are rather meso between corner-protonated and edge-protonated ideals. We will use the PCP⁺ label for any closed structure, in which case the label can apply to *both* intermediates and transition states. For the dialkyl PCP⁺ structures important in this study, we will refer to the base and the sides of the PCP⁺ unit, as shown in Table 1.

For the first 3 + 3 + 4.8 ps of simulation time, the *sec*-nonenium ion explored only open structures. Significant chemisorption (>50 fs) to the weakly nucleophilic chloroaluminate anions never occurred. Table 1 summarizes the important observations from the reverse-annealing simulation.

Using the AIMD results as a guide, we also did calculations to identify the 0 K potential-energy-surface (PES) intermediates and transition states for the two-step reaction observed. For these optimizations, the solvent molecules were removed from the simulation cell and replaced with a homogeneous negative background charge, to avoid the difficulty of optimizing “soft” modes of a quenched molecular liquid. A conjugate gradient algorithm was used to determine the geometries of intermediates, and the transition-state geometries were determined using the dimer method²¹ as recently improved by Heyden et al.²² One vibrational mode with imaginary frequency was verified for each transition state configuration. In all optimized structures (see Supporting Information), the maximal force acting on ions (nuclei) was smaller than 0.04 eV/\AA .

The first step (near $t = 4932 \text{ fs}$) of the observed two-step reaction is described in Figure 1. Both intermediates, as well as the transition state, possess closed structures with a common planar CCCH moiety. From our optimization calculations, using the particular nonenium conformations observed in the simulated step, we found an E_a barrier of 43 kJ mol^{-1} and a ΔE of -1 kJ mol^{-1} (no zero-point corrections applied). This step was first discovered computationally by Corma and co-workers (their A \rightarrow B \rightarrow C) for the 2-pentenium ion, for which $E_a = 34$ and $\Delta E = -8 \text{ kJ mol}^{-1}$ from their B3P86/6-31G(d) calculations.³ Dumesic and co-workers also optimized very similar transition states (their TS6 and TS7) for further one-step branching of already-branched 2-methylpentenium ions, even when in contact with an oxide catalyst fragment.⁴

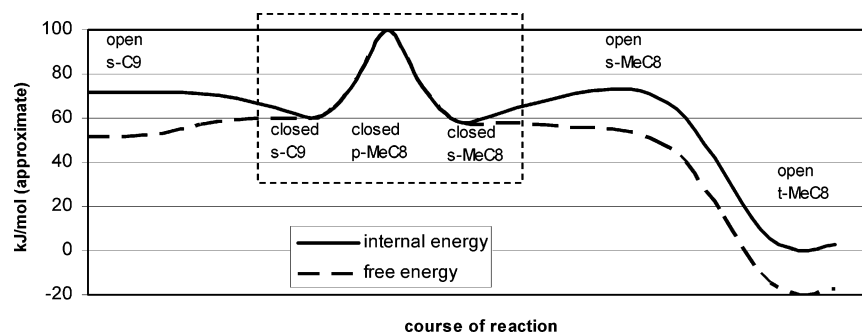


Figure 3. Crude sketch of the internal energy and free energy of a branching isomerization from nonenium ion to methyloctenium ion. The region of closed structures (containing the step we call step 1) is enclosed within a dashed rectangle. The sketch includes a very crude estimate of 20 kJ mol^{-1} for the entropic lowering of open-structure energies relative to closed-structure ones, to account for the spontaneous opening of closed structures in the 800 K simulation.

The second step (near $t = 5258$ fs) is described in Figure 2. Here, as in the first step, a structural adjustment is required to achieve the transition state, before the H-atom transfer can occur to complete the step. From our optimization calculations, we found $E_a = 17$ and $\Delta E = -57$ kJ mol⁻¹. This step was also found by Corma and co-workers (their C → D → E) for the 2-pentenium ion, for which $E_a = 17$ and $\Delta E = -61$ kJ mol⁻¹ from their B3P86/6-31G(d) calculations.³

The AIMD simulation thus confirms that the two steps presented by ref 3 represent a statistically probable route for the branching transformation. However, the simulation also gives us a better “feel” for the process and gave us two valuable insights into this isomerization. The first is our new description of the critical first step as being entirely composed of PCP⁺ structures. Reference 4 correctly noted difficulties in equating this first step with the traditionally cited mechanism of Brouwer.^{2,23,24} Instead, the mechanism of Edwards and Lesage²⁵ (their A → E → B for the branching of a cyclohexanone cation) is the best of the early predictions: not only is it entirely composed of PCP⁺ structures, but the two C–C bonds they draw as stretched in each of their structures (A, E, and B) are the correct ones, according to the DFT-optimized structures. We felt that drawing only one C–C bond as dotted, instead of two as in Edwards and Lesage, would allow a more comforting description of these intermediate and transition-state structures as “closed secondary” and “closed primary” carbenium ions, respectively.

The second new insight is with regard to the opening and closing of secondary carbenium ions. This simulation demonstrated that open structures are far more prevalent than closed ones. This does not fit well with the original comparisons by Sieber et al. for the 2-butyl ion,²⁰ which calculated PES energies within 5 kJ mol⁻¹ for the two forms, with a non-negligible (though undetermined) barrier between the two. Suspecting that the preference for open forms was either due to entropy or to solvation, we performed an 800 K (Andersen thermostat²⁶) AIMD calculation on a secondary nonenium ion in a continuum negative background charge for 7.5 ps. The initially closed structure quickly opened and stayed open most (>80%) of the time, suggesting an entropy effect. Upon ensuing minimization, the structure became pseudo-closed ($\theta_{\text{CCC}} = 95^\circ$). Hence, although the internal energy of the open form appears to be higher than that of the closed (PCP⁺) form, its free energy appears to be lower at 800 K, at least for the particular conformations sampled during our runs. Our updated description of this situation appears in Figure 3, with the caveat that the two presented energy surfaces are necessarily crude, due to the numerous possible anti/gauche positions of the alkyl arms.

Acknowledgment. The supercomputer in Regina was funded by the Canada Foundation for Innovation and the Government of Saskatchewan. Operating funds were provided by the Natural Sciences and Engineering Research Council of Canada, the Austrian Science Funds and the Center for Computational Materials Science (University of Vienna).

Supporting Information Available: Cartesian coordinates of five optimized C₉H₁₉⁺ geometries (three minimum-energy and two transition-state ones). This material is available free of charge via the Internet at <http://pubs.acs.org>.

References and Notes

- (1) McCaulay, D. A. *J. Am. Chem. Soc.* **1959**, *81*, 6437.
- (2) Brouwer, D. M.; Hogeveen, H. *Prog. Phys. Org. Chem.* **1972**, *9*, 179.
- (3) Boronat, M.; Viruela, P.; Corma, A. *J. Phys. Chem.* **1996**, *100*, 16514.
- (4) Natal-Santiago, M. A.; Alcalá, R.; Dumesic, J. A. *J. Catal.* **1999**, *181*, 124.
- (5) Demuth, T.; Rozanska, X.; Benco, L.; Hafner, J.; van Santen, R. A.; Toulhoat, H. *J. Catal.* **2003**, *214*, 68.
- (6) Unbiased simulations of chemical reactions are rare, because of limited simulation times. Recent MD studies of organic reactions have invoked advanced techniques, such as thermodynamic integration⁷ and metadynamics,^{8–10} which require a priori choice of a reaction coordinate.
- (7) Fleurat-Lessard P.; Ziegler, T. *J. Chem. Phys.* **2005**, *123*, 084101.
- (8) Cucinotta, C. S.; Ruini, A.; Catellani, A.; Stirling, A. *J. Phys. Chem. A* **2006**, *110*, 14013.
- (9) Lee, J.-G.; Ascuitto, E.; Babin, V.; Saguí, C.; Darden, T.; Roland, C. *J. Phys. Chem. B* **2006**, *110*, 2325.
- (10) Stirling, A.; Iannuzzi, M.; Laio, A.; Parrinello, M. *Chem. Phys. Chem.* **2004**, *5*, 1558.
- (11) Kresse, G.; Furthmüller, J. *J. Phys. Rev. B* **1996**, *54*, 11169.
- (12) Perdew, J. P.; Chevary, J. A.; Vosko, S. H.; Jackson, K. A.; Pedersen, M. R.; Singh, D. J.; Fiolhais, C. *Phys. Rev. B* **1992**, *46*, 6671.
- (13) Blöchl, P. E. *Phys. Rev. B* **1994**, *50*, 17953.
- (14) Kresse, G.; Joubert, D. *Phys. Rev. B* **1999**, *59*, 1758.
- (15) Vanderbilt, D. *Phys. Rev. B* **1990**, *41*, 7892.
- (16) Kresse, G.; Hafner, J. *J. Phys. Condens. Matter* **1994**, *6*, 8245.
- (17) Xiao, L.; Johnson, K. E.; Treble, R. G. *J. Mol. Catal. A* **2004**, *214*, 121.
- (18) Nosé, S. *J. Chem. Phys.* **1984**, *81*, 511.
- (19) Allen, M. P.; Tildesley, D. J. *Computer Simulations of Liquids*; Clarendon: Oxford, U.K., 1987.
- (20) Sieber, S.; Buzek, P.; Schleyer, P. v. R.; Koch, W.; Carneiro, J. W. de M. *J. Am. Chem. Soc.* **1993**, *115*, 259.
- (21) Henkelman, G.; Jonsson, H. *J. Chem. Phys.* **1999**, *111*, 7010.
- (22) Heyden, A.; Bell, A. T.; Keil, F. K. *J. Chem. Phys.* **2005**, *123*, 224101.
- (23) Sie, S.T. Isomerization Reactions. In *Handbook of Heterogeneous Catalysis*; Ertl, G., Knozinger, H., Weitkamp, J., Eds.; VCH Wiley: Weinheim, Germany, 1997; Vol. 4, pp 1998–2017.
- (24) Ono, Y. *Catal. Today* **2003**, *81*, 3.
- (25) Edwards, O. E.; Lesage, M. *Can. J. Chem.* **1963**, *41*, 1592.
- (26) Andersen, H. C. *J. Chem. Phys.* **1980**, *72*, 2384.